Ultrafast Carrier Relaxation in Si Studied by Time-Resolved Two-Photon Photoemission Spectroscopy: Intravalley Scattering and Energy Relaxation of Hot Electrons

T. Ichibayashi and K. Tanimura

The Institute of Scientific and Industrial Research, Osaka University, 8-1 Mihogaoka, Ibaraki, Osaka 567-0047, Japan

(Received 6 June 2008; published 26 February 2009)

The dynamical relaxations of photogenerated hot carriers in the X valley of Si have been studied using time-resolved two-photon photoemission spectroscopy. Intravalley scattering is completed within 100 fs to form a quasiequilibrated electron distribution near the conduction-band minimum, while maintaining about half the excess energy given to hot electrons. The energy relaxation follows the scattering with a 240-fs time constant that is independent of the excess energy.

DOI: 10.1103/PhysRevLett.102.087403 PACS numbers: 78.47.J−, 73.20.At, 78.55.Ap, 79.60.Bm

The continuing miniaturization of semiconductor devices into the nanoscale regime requires a clear understanding of the ultrafast carrier dynamics near surfaces at an increasingly shorter time scale. Several striking structural effects caused by fs-laser interactions with semiconductors [1–3] have emphasized the importance of a comprehensive understanding of ultrafast carrier relaxation to elucidate the mechanisms involved. The carrier dynamics in Si, one of the most important semiconductors and the foundation of modern electronic devices, has been studied extensively using time-resolved optical techniques that detect induced changes in dielectric functions because of the indirect band gap [4,5]. These optical methods require complicated fitting procedures, assumptions and approximations to deconvolve the underlying and/or sequential processes. Therefore, quantitative evaluation of the primary dynamical processes remains essentially indirect; unambiguous quantitative understanding of ultrafast carrier dynamics in Si has not yet emerged.

In this Letter, we present a comprehensive study of the relaxation of hot electrons excited into the X valley in Si using time-resolved two-photon photoemission spectroscopy (2PPE) with tunable fs-pump pulses. We overcome several impediments discussed previously [6–11] and characterize the ultrafast dynamics in terms of a time-resolved electron distribution function (TR-EDF) of bulk-conduction electrons. We describe three unique achievements: the first determination of intravalley electron thermalization time [12], the direct measurement of the energy relaxation time, and the first evaluation of the photon energy dependence of the maximum electron temperature.

Boron-doped p-type Si(001) and Si(111) wafers (10 Ω cm) were clamped with Ta sheets to the sample holder in an ultrahigh vacuum chamber ($<5 \times 10^{-11}$ Torr). Scanning tunneling microscopy characterization showed that the (100) surfaces were well ordered double-domain (2×1) structures with typical surface-defect concentration n_D of 1% and (111) surfaces were almost perfect (7×7) structures, with n_D less than 0.01%. A 250-kHz regeneratively amplified Ti-sapphire laser, operated between 760 and 830 nm, was used to pump an optical parametric amplifier to generate pump pulses (100 fs) with a pump-photon energy $h\nu_{\mathrm{pump}}$ ranging from 1.8 to 2.6 eV. The probe pulses of 150-fs width were generated by frequency tripling or quadrupling the regenerative amplifier output using nonlinear crystals. The pump and probe pulses with a preset time delay (Δt) were aligned coaxially and focused on the sample surfaces at 45° to normal. The probe pulse was p polarized while the pump pulses could be selected to be either s or p polarized. Electrons emitted along the surface normal (±2°) were analyzed by a hemispherical analyzer with an energy resolution of 70 meV. The axis of energy E in all photoemission spectra is scaled with respect to the valence band maximum (VBM) using well established values for ionization energy and work function [10,11].

We first discuss results for Si(001)-(2×1) to differentiate our results from those in previous 2PPE studies [7,8]. Figure 1 displays a typical 2PPE spectra measured at 296 K with $h\nu_{\mathrm{pump}}$ of 2.03 eV. The asymmetric Si surface dimers form two surface electronic bands: a filled dangling-bond band (D_{up}) and an empty band (D_{down}) [11,13]. In Fig. 1, the peak at 1.90 eV is due to coherent two-photon photoemission from the D_{up}, excited only for p-polarized pump and probe pulses, and the peak at 0.68 eV originates from D_{down} at the $\bar{\Gamma}$ point [10,11]. The D_{down} state is transiently populated, reaching a maximum intensity at $\Delta t = 1$ ps. The clear detection of the intrinsic surface peaks confirms the well-ordered atomic structures of surfaces and ensures the reliability of quantitative analysis of the spectra.

As shown in the inset at a magnified scale, we observe a small but clearly resolved peak near the conduction band minimum (CBM, $E = 1.12$ eV). For $\Delta t > 200$ fs, the spectral shape of the peak evolves progressively and converges to a center energy of 1.14 eV. The peak shape remains the same for $\Delta t > 1$ ps. The 1.14-eV peak has been identified as the CBM photoemission induced by the surface photoelectric effect via the inverse LEED (low-energy electron diffraction) state which serves as the final state for photoemission [14]. The relatively small yield of the CBM peak is due to its evanescent character [6,14].

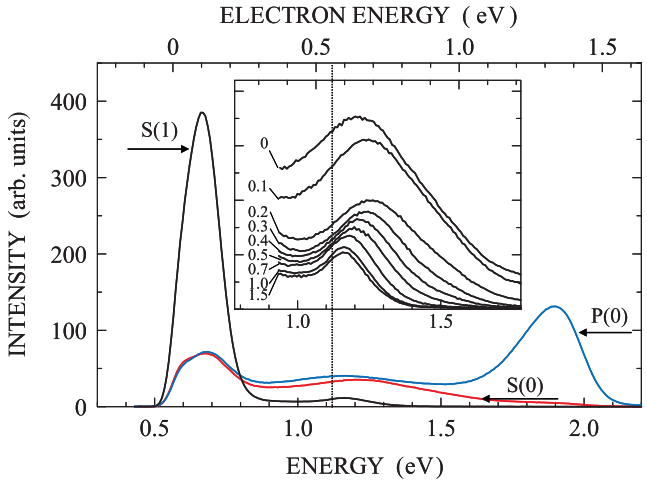

FIG. 1 (color). Time-resolved 2PPE spectra for Si(001)-(2 × 1) measured by a 2.03-eV pump (fluence of 520 μJ cm^{-2}) and 4.89-eV probe pulses. The curve labeled $P(0)$ is for p-polarized pump pulses with $\Delta t = 0$, while those labeled S(0) and S(1) are for s-polarized pump pulses with $\Delta t = 0$ and 1 ps, respectively. The dotted line shows the energy position of the CBM. The inset shows the temporal evolution of the photoemission near the CBM measured at Δt's indicated by numbers in ps under s-polarized pump pulses. The upper axis represents the electron energy measured from the low-energy cutoff representing vacuum level.

Nevertheless, a clear progressive change in the spectral shape provides direct spectroscopic evidence of femtosecond dynamical relaxation of hot electrons in Si.

Because of the indirect band gap, photoexcitation at a given $h\nu_{\text{pump}}$ of Si can induce many phonon-assisted indirect transitions. In such a case, the hot holes and electrons are presumed to equally share the excess energy usually defined as the difference between $h\nu_{\text{pump}}$ and the band gap energy E_g [5]. Then, photogenerated electrons are placed around E^e_{ex} above the CBM in the X valley, and may form a broad peak, where E^e_{ex} is the electron excess energy defined here by $(h\nu_{\text{pump}}\text{-}E_g)/2$. At $\Delta t = 0$, a broad peak around 1.2 eV dominates over other features. However, the peak energy is much lower than E^e_{ex} for 2.03-eV excitation ($E^e_{\text{ex}} = 0.45$ eV), and it becomes even lower than the CBM position for excitation at $h\nu_{\text{pump}}$ less than 2 eV. Therefore, the initial broad peak is not related to the real electron population in the X valley, but is a coherent two-photon peak (CP) associated with some intermediate states.

Although the CP still dominates other features at $\Delta t = 100$ fs, an abrupt intensity drop between $\Delta t = 100$ and 200 fs indicates qualitative changes in the photoemission process. At $\Delta t = 200$ fs, the peak energy shifts to higher energy from that at $\Delta t = 0$ fs, indicating a relative growth of the high-energy peak due to real-state populations. To characterize the onset of relaxations of real state populations, we analyzed temporal changes in the photoemission intensity Ip around the CBM peak. The open circles in Fig. 2 show the change in Ip at $E = 1.5$ eV that probes the population at 0.38 eV above the CBM. When compared with the cross correlation between pump and probe pulses (shown by the red curve) that represents an independent measure of zero time delay, a short-lived real-population component is evident by a persistent decay at $\Delta t > 0.2$ ps. A finite delay (~45 fs) of the peak of Ip is indicative of a finite formation time of similar magnitude [15]. We model the temporal change as a superposition of a CP component (dashed curve) and a real-population component (RP, blue curve) using a rate-equation model. The electrons photoexcited at E^e_{ex} above the CBM with the density n^* are relaxed to near the CBM to populate an electron density n at 0.38 eV above the CBM with the formation time τ_f, and n is reduced further with a time constant τ_d by a subsequent relaxation process. Then, $dn^*/dt = g(t) - (1/\tau_f)n^*$, and $dn/dt = (1/\tau_f)n^* - (1/\tau_d)n$, where $g(t)$ is a generation term that accounts for the pump-pulse shape. At $\Delta t > 0.2$ ps, where overlap between pump and probe pulses can be neglected, the Ip decreases with τ_d of 100 ± 10 fs. Then, the best-fit procedure, with two parameters (the ratio between CP and RP and τ_f), indicates that $\tau_f = 40 \pm 10$ fs, leading to a maximum population 100 fs after excitation. We conclude that the blue curve in Fig. 2 represents the dynamics of hot electrons accumulated near the CBM, monitored at 0.38 eV above the CBM. The τ_f of 40 ± 10 fs may represent the rate of intravalley relaxation including momentum-relaxing scattering. The hot electron system thus formed undergoes energy relaxation within 1 ps.

In order to prove that the observed features are characteristic of bulk Si, we conducted similar measurements on

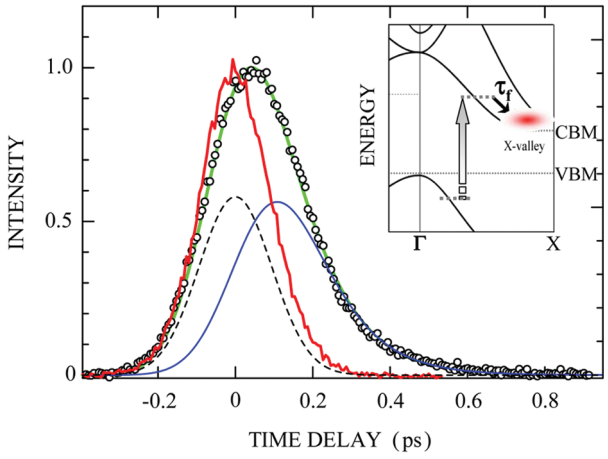

FIG. 2 (color). Temporal change in photoemission intensity I_P measured at $E = 1.50$ eV for s-polarized pump pulses, the open circles, and the cross correlation between pump and probe pulses, the red curve, evaluated from the temporal changes of the D_{up} peak. The dashed and blue curves are the two components of the I_P, resolved by the analysis using a rate-equation model (see text), and the solid green curve (through the open circles) is the sum of the two. The inset shows a schematic representation of the process analyzed by the rate-equation model.

Si(111)-(7 × 7), which has metalliclike surface electronic bands: a filled band (S_1) and an empty band (U_1) [13]. To show these features are general at any temperature, Fig. 3 displays a series of 2PPE spectra measured at 90 K under a flat-band condition by using the photovoltaic effect [16]. The low energy part of the spectra ($E < 1$ eV) represents transient changes of the temporally occupied U_1 band. Additionally, there are peaks forming near the CBM, clearly evident at $\Delta t > 300$ fs. These peaks evolve rapidly and converge to a center energy of 1.20 eV, which has been identified as the CBM peak for this surface at 90 K [14]. The spectral shapes of the CBM peak at representative time delays, displayed in the inset, show essentially the same temporal evolution in their widths and peak energies as those for Si(001)-(2 × 1). The CBM peak measured at 296 K also shows a similar temporal evolution. Furthermore, analysis similar to that in Fig. 2 has given the same value of τ_f, substantiating the intrinsic nature of hot electron relaxation near the CBM.

To quantify the relaxation process, it is crucial to determine the TR-EDFs by overcoming several issues. The first issue concerns the energy (ε) dependence of photoemission efficiency $\eta(\varepsilon)$, since the transition dipole moments between a temporally populated state and the crystalline Bloch states as the final states for photoemission depend on ε [9]. In the present case, inverse LEED states, which serve as the final state, have not been fully characterized theoretically for Si surfaces. We examined experimentally the $\eta(\varepsilon)$ in the range about 1 eV above the vacuum level Φ_{vac}, by measuring the photoemission spectra at a given Δt

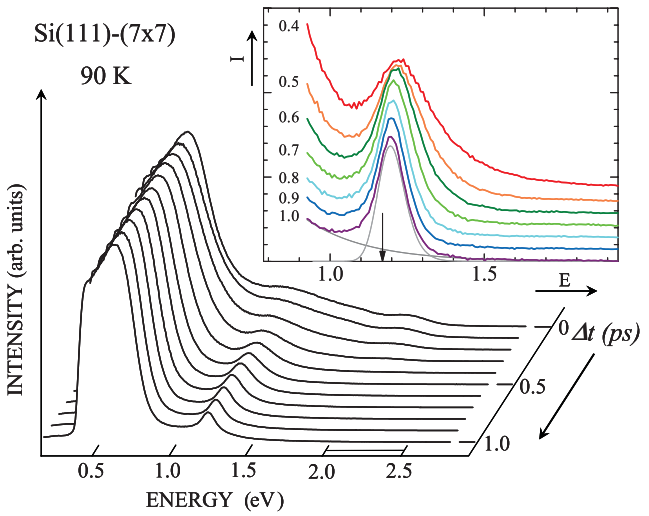

FIG. 3 (color). A series of 2PPE spectra measured for Si(111)-(7 × 7) at 90 K for *s*-polarized 2.21-eV pump pulses and *p*-polarized 4.95-eV probe pulses. The inset shows the temporal evolution of the CBM peak in an expanded scale from $\Delta t = 0.4$ ps to 1 ps. The arrow shows the energy position of the CBM (1.17 eV at 90 K). The grey curves associated with the $\Delta t = 1.0$ ps spectrum are the results of spectral analysis including a high-energy tail from the U_1 band and a convoluted EDF with an electron temperature of 300 K.

under the same pump-pulse conditions using probe pulses with different photon energies $h\nu_{\text{prob}}$ (4.89–6.00 eV). When normalized with respect to electron energy, by adjusting for differences in $h\nu_{\text{prob}}$, all spectra show the same characteristic shape. Furthermore, when compared at an equivalent probe laser photon flux, the intensities are the same within experimental error. This demonstrates that for the "energy window" about 1 eV above Φ_{vac}, with a width of about 1 eV, the $\eta(\varepsilon)$ is constant; the observed spectra directly determine TR-EDFs.

A second issue is the possible distortion of photoemission spectral shapes due to surface defects. The inverse LEED state is surface sensitive, and surface defects may produce strong effects on photoemission spectra via elastic and/or inelastic scattering upon photoemission. In fact, a CBM spectrum from Si(001)-(2 × 1) with 1% of n_D is wider than that from Si(111)-(7 × 7) with less than 0.01% of n_D [15]. This difference may be due to surface defects [17]. To avoid possible errors in quantitative analysis, we restrict our discussion to the results for Si(111)-(7 × 7) with the smaller n_D.

Since the photogenerated carrier density ($< 1 \times 10^{18}/\text{cm}^3$) is much less than the effective density of states of the conduction band, we can simulate the band shape using a Boltzmann distribution function with an effective electron temperature T^*, convolved with the 70-meV instrument resolution. An example of the simulation is shown by grey curves representing an electron distribution function (EDF) with $T^* = 300$ K and a U_1-band tail for the spectrum at $\Delta t = 1.0$ ps in the inset of Fig. 3. Also, the spectrum at $\Delta t = 10$ ps (not shown) is characterized with $T^* = 275$ K, which is exactly the same as that determined for the quasiequilibrated surface S_1/U_1 band under a flat-band condition [14]. Therefore, T^* may be reasonably deduced by spectral-shape analysis [18].

In Fig. 4, we show a temporal change of T^* at 296 K; it decreases exponentially with a time constant of 240 fs (solid curve) to reach the equilibrated temperature at $\Delta t = 2$ ps. The result provides the first experimental proof of an exponential energy relaxation process of hot electrons in Si and gives direct indication of the energy relaxation process of the quasiequilibrated hot electrons. The inset of Fig. 4 shows the average energy $E_{\text{av}}(= 3/2k_BT^*)$ given by T^* extrapolated at $\Delta t = 100$ fs, where the electron density near the CBM forms the maximum, displayed in Fig. 2. Because of a strong overlap between the CP and RP peaks, it was not possible to analyze the CBM-peak spectra at $\Delta t < 300$ fs for raw spectral data. However, the spectra obtained by point-by-point deconvolution (Fig. 2) could be reasonably described by an EDF of T^* extrapolated in Fig. 4. Therefore, the value in the inset represents the maximum internal energy of quasiequilibrated hot electrons via intravalley scattering. It increases with $h\nu_{\text{pump}}$, showing that the energy initially given to the hot electrons is partially maintained in this relaxation process. However, the E_{av} is less than 1/2 of E_{ex}^e, indicating that more than

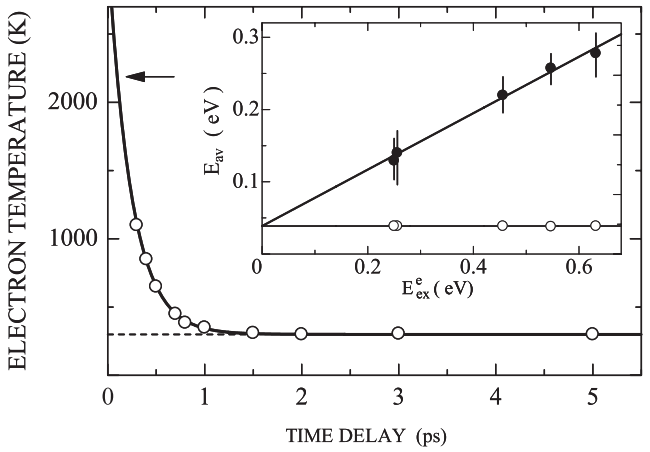

FIG. 4. The electron temperature as a function of Δt for 2.21-eV excitation. The solid curve is the fit of a single exponential-decay component and a constant value (296 K). The time constant is 240 ± 20 fs. The inset shows the average energy, E_{av}, at 100 fs, (solid circles) and at 2 ps, (open circles) after excitation as a function of electron excess energy, E^e_{ex}, given by half the difference between $h\nu_{\mathrm{pump}}$ and E_g for Si(111)-(7×7) at 296 K. The error bars are estimated maximum errors evaluated from the average of several measurements under similar conditions.

half the electron excess energy is transferred to the lattice within 100 fs during intravalley relaxation. This reveals an ultrafast lattice heating effect and the important role of electron-phonon (e-p) interactions in electronic thermalization in Si.

The excess-energy dependence of τ_{el} was studied by Monte Carlo calculations [19], and the previous results were discussed based on this context [5]. On the other hand, we found that τ_{el} is constant irrespective of $h\nu_{\mathrm{pump}}$; it is 240 fs $\pm$ 10 fs at 296 K for $E^e_{\mathrm{ex}} < 0.62$ eV. In view of the results revealed here, the independency of τ_{el} may be a natural consequence, since the intravalley scattering time is short compared to τ_{el} and the energy relaxation is primarily governed by e-p interaction of quasiequilibrated hot electrons formed near the CBM. We find that the magnitude of τ_{el} depends on sample temperature T; it becomes 310 ± 10 fs at 90 K, irrespective of $h\nu_{\mathrm{pump}}$. Since the rate of e-p interaction depends on T via phonon-occupation number $n(T)$ as $(2n(T) + 1)$ [20], the result shows that the energy $\hbar\omega$ of phonons governing the energy relaxation must satisfy the relation; $(2n(90) + 1)/(2n(296) + 1) = 0.77$. This tells us that 52-meV phonons are primarily responsible for the process. This value is close to the LO phonon energy at the X point (53.5 meV) of Si, thus substantiating strongly our conclusion. Therefore, the intravalley relaxation of hot electrons in Si is characterized by a fast formation of quasiequilibrated electron systems near the CBM and a common energy relaxation process characterized by τ_{el}.

This work was supported by a Specially Promoted Research of Grant-in-Aid for Scientific Research from the Ministry of Education, Science, Technology, Sports, and Culture of Japan.

[1] A. Rousse *et al.*, Nature (London) **410**, 65 (2001).
[2] P. B. Hillyard *et al.*, Phys. Rev. Lett. **98**, 125501 (2007).
[3] M. Harb *et al.*, Phys. Rev. Lett. **100**, 155504 (2008).
[4] T. Sjodin *et al.*, Phys. Rev. Lett. **81**, 5664 (1998); Chem. Phys. **251**, 205 (2000).
[5] A. J. Sabbah and D. M. Riffe, Phys. Rev. B **66**, 165217 (2002).
[6] P. J. Feibelman and D. E. Eastman, Phys. Rev. B **10**, 4932 (1974).
[7] J. R. Goldman and J. A. Prybyla, Phys. Rev. Lett. **72**, 1364 (1994).
[8] S. Jeong and J. Bokor, Phys. Rev. B **59**, 4943 (1999).
[9] S. Ramakrishna, F. Willing, and A. Knorr, Appl. Phys. A **78**, 247 (2004).
[10] C. Kentsch *et al.*, Phys. Rev. B **65**, 035323 (2001).
[11] M. Weinelt *et al.*, Phys. Rev. Lett. **92**, 126801 (2004); Appl. Phys. A **80**, 995 (2005).
[12] The ionization energy of Si(100) surfaces is 5.40 ± 0.03 eV (Ref. [10]). Since the band-gap energy is 1.12 eV at 300 K, one needs $h\nu_{\mathrm{prob}}$ greater than 4.3 eV for the CBM photoemission. However, the $h\nu_{\mathrm{prob}}$ used in Ref. [7] is only 4 eV. Therefore, the photoemission spectra in Ref. [7] are due to surface defect states and/or the two-photon photoemission. Although $h\nu_{\mathrm{prob}}$ of 4.66 eV is used in Ref. [8], the pronounced photoemission peak has been attributed to surface defect states.
[13] W. Mönch, *Semiconductor Surfaces and Interfaces* (Springer, Berlin, 1995).
[14] T. Ichibayashi and K. Tanimura, Phys. Rev. B **75**, 235327 (2007).
[15] H. Ueba and B. Gumhalter, Prog. Surf. Sci. **82**, 193 (2007).
[16] M. Mauerer, I. L. Shumay, W. Berthold, and U. Höfer, Phys. Rev. B **73**, 245305 (2006).
[17] Surface defect scattering of photoelectrons may induce an additional broadening of the peaks as the primary effect. Analysis of the CBM photoemission with 120-meV convolution for Si(001)-(2×1) gave the same quantitative results as those for Si(111)-(7×7) that are described in the text.
[18] To exclude ambiguities in determining T^*, due to a considerable overlap of the CBM peak with the high-energy tail of surface-state photoemissions, we compared the peak energy of a CBM photoemission band, which is much less affected by overlap with the structureless surface-band tail. When convoluted, the EDFs show clear peaks that depend sensitively upon T^*, providing another way to determine T^*. The temperatures evaluated from spectral-shape fitting in Fig. 4 were confirmed to be consistent with those determined by the peak-energy analysis.
[19] E. Constant, in *Hot-Electron Transport in Semiconductors*, edited by L. Reggiani (Springer-Verlag, New York, 1985), p. 227.
[20] B. K. Ridley, *Quantum Processes in Semiconductors* (Oxford University Press, Oxford, 1988).